Journal of Biotechnology 335 (2021) 65–75

Contents lists available at ScienceDirect

Journal of Biotechnology

journal homepage: www.elsevier.com/locate/jbiotec

Automation of high CHO cell density seed intensification via online control of the cell specific perfusion rate and its impact on the N-stage inoculum quality

Markus Schulze [a,b,*], Johannes Lemke [a], David Pollard [c], Rene H. Wijffels [b,d], Jens Matuszczyk [a], Dirk E. Martens [b]

[a] Corporate Research, Sartorius Stedim Biotech GmbH, August-Spindler-Str. 11, 37079, Göttingen, Germany
[b] Bioprocess Engineering, Wageningen University, PO Box 16, 6700 AA, Wageningen, The Netherlands
[c] Corporate Research, Sartorius Stedim North America, 6 Tide Street, Boston MA, 02210, United States
[d] Biosciences and Aquaculture, Nord University, N-8049 Bodø, Norway

ARTICLE INFO

Keywords:
Process intensification
N-1 perfusion
Capacitance
Online control
Cell-specific perfusion rate (CSPR)
CHO cell culture

ABSTRACT

Current CHO cell production processes require an optimized space-time-yield. Process intensification can support achieving this by enhancing the productivity and improving facility utilization. The use of perfusion at the last stage of the seed train (N-1) for high cell density inoculation of the fed-batch N-stage production culture is a relatively new approach with few industry applicable examples. Within this work, the impact of the cell-specific perfusion rate (CSPR) of the N-1 perfusion and the relevance of its control for the quality of generated inoculation cells was evaluated using an automated perfusion rate (PR) control based on online biomass measurements. Precise correlations ($R^2 = 0.99$) between permittivity and viable cell counts were found up to the high densities of $100{\cdot}10^6$ c·mL^{-1}. Cells from N-1 perfusion were cultivated at a high and low CSPR with 50 and 20 pL·(c·d)$^{-1}$, respectively. Lowered cell growth and an increased apoptotic reaction was found as a consequence of the latter due to nutrient limitations and reduced uptake rates. Subsequently, batch cultivations (N-stage) from the different N-1 sources were inoculated to evaluate the physiological state of the inoculum. Successive responses resulting from the respective N-1 condition were uncovered. While cell growth and productivity of approaches inoculated from high CSPR and a conventional seed were comparable, low CSPR inoculation suffered significantly in terms of reduced initial cell growth and impaired viability. This study underlines the importance to determine the CSPR for the design and implementation of an N-1 perfusion process in order to achieve the desired performance at the crucial production stage.

1. Introduction

Mammalian cell lines are the predominantly used host for the production of different recombinant therapeutic proteins (Jayapal et al., 2007) primarily being monoclonal antibodies (mAbs) (Kunert and Reinhart, 2016). Recently, continuous biomanufacturing applying process intensification of upstream processes has received much attention due to its ability to further optimize current state-of-the art mAb production capabilities (Bielser et al., 2018; Karst et al., 2018). By convention, the upstream process starts with cell expansion after cell thaw from a cell bank through multiple batch-wise passages from mL to hL scale during the seed train. At its end (N-1 stage) cells are sufficiently propagated for inoculation of the production bioreactor (N-stage). Currently, fed-batch (FB) processes in stirred tank reactors are predominantly used in the biomanufacturing industry at the N-stage up to m^3-scales (Ecker and Ransohoff, 2014; Kantardjieff and Zhou, 2014).

However, since more and more drugs are going off-patent (Blackstone and Joseph, 2013) and the global world population grows both in age and number (United Nations, Department of Economic and Social Affairs, Population Division, 2019), production of biopharmaceuticals

Abbreviations: CHO, Chinese hamster ovary; CSPR, cell-specific perfusion rate; FB, fed-batch; IgG, Immunoglobulin G; mAb, monoclonal antibody; PAT, process analytical technologies; PR, perfusion rate; RM, rocking motion.

* Corresponding author at: Sartorius Corporate Research, Sartorius Stedim Biotech GmbH, August-Spindler-Str. 11, 37079, Göttingen, Germany.
E-mail address: markus.schulze@sartorius.com (M. Schulze).

https://doi.org/10.1016/j.jbiotec.2021.06.011
Received 19 February 2021; Received in revised form 25 May 2021; Accepted 1 June 2021
Available online 4 June 2021

must become even more efficient and flexible. Implementing process intensification in upstream processes can help in achieving this. It allows for a reduction of equipment size, an improved throughput of processes as well as to increase their efficiency (Ponce-Ortega et al., 2012). In the past, the biopharmaceutical industry made significant progress in process intensification due to cell line engineering, media development and improved process control mainly for conventional biomanufacturing. Nowadays, more attention is paid to the process strategies itself including perfusion to further intensify mammalian bioprocesses in terms of enhanced volumetric productivities and increased manufacturing flexibility (Bielser et al., 2018). Recent studies revealed at least doubled productivities (Gagnon et al., 2019) and even reported 8-fold titer increases in intensified N-stage production processes (Xu et al., 2020b).

Perfusion processes are characterized by a continuous media exchange while cells are retained inside the bioreactor by a cell retention device, e. g. filters (Clincke et al., 2011; Karst et al., 2016). As nutrients are continuously provided and potentially inhibiting metabolites, like ammonia and lactate, are washed out from the perfusion bioreactor, the cells are continuously exposed to the most favorable conditions at which a steady-state in terms of metabolite concentrations, osmolality and other process parameters is established. Thus, both cell growth and protein production can be intensified compared to conventional biomanufacturing. A perfusion process can thus be applied in the seed train to generate inoculum for the N-stage or it can be applied as an N-stage production processes. The latter one strives to continuously produce product, up to 60 days (Warikoo et al., 2012), often using a constant cell removal rate in order to maintain a constant, moderate viable cell concentration (VCC). This strategy for continuous expression is not only used in mammalian, but was recently successfully applied to insect cell culture as well (Fernandes et al., 2021). Also, there are several examples about concentrated fed-batches (Yang et al., 2016) and hybrid N-stage processes using a combination of perfusion and fed-batch (Hiller et al., 2017). In contrast, the aim of a seed train using perfusion is to generate very high VCCs for the inoculation of a subsequent N-stage process. This kind of intensification allows to significantly reduce the number of seed stages and the equipment size required. For example a fed-batch with a seeding concentration of $0.3{\cdot}10^6$ c·mL^{-1} inoculated from an N-1 perfusion with $100{\cdot}10^6$ c·mL^{-1} allows for a 33 times reduction in reactor size at the N-1 stage as compared to using a conventional N-1 process with $3{\cdot}10^6$ c·mL^{-1}. This increases flexibility and improves efficiency. In perfusion processes whether for protein production or inoculum generation, one very important critical process parameter is the cell-specific perfusion rate (CSPR), i. e. the volumetric rate the bioreactor is perfused with fresh media in relation to the VCC. The identification of the CSPR is critical to establish during the development of a perfusion process (Konstantinov et al., 2006). Defining the minimal CSPR allows to optimize expensive media utilization, thus keeping the cost of goods low (Xu et al., 2017). Ideally, control of the optimum CSPR during the process is accomplished by using online biomass measurements with for example a capacitance probe and feedback control to adjust the perfusion rate (PR) automatically. There are several references about such applications in intensified processes (Karst et al., 2016; Warikoo et al., 2012; Yang et al., 2014), but reliable online biomass measurements up to $100{\cdot}10^6$ c·mL^{-1} have not been demonstrated so far.

A critical issue of applying online biomass measurements to N-1 perfusion is the need for accuracy to avoid potential imprecision of incorrectly setting the PRs based on a CSPR setpoint. This would rapidly cause potential misfeeding and is particularly critical towards the end of the process when achieving high VCCs ($100{\cdot}10^6$ c·mL^{-1}). This could potentially impair the quality of the generated cells for the subsequent N-stage inoculation, i. e. cell growth and ultimately its mAb product yield and quality. Hence, the precise online biomass measurement in N-1 perfusion processes is critical.

Therefore, this study focuses on two objectives. Firstly, the technical ability to control the PR in an N-1 perfusion process precisely up to $100{\cdot}10^6$ c·mL^{-1} based on an online biomass sensor. Secondly, utilizing this control to apply two different CSPRs (low and high) in this process. The impact of this parameter on cellular responses at the N-1 perfusion in terms of cell growth, metabolic rates and apoptotic reactions were investigated. On this basis, batch cultivations were inoculated as N-stage representatives using differently conditioned cells generated from conventional and intensified N-1 stages and were measured regarding cell growth, productivity and product quality. Thus, translation of cellular responses from N-1 into N-stage were evaluated, ultimately demonstrating the relevance of precise and reliable online PR control.

2. Materials and methods

2.1. Cell lines and medium

The CHO cell line (DG44, Sartorius) used in this study expressed a monoclonal antibody (IgG1). All media and feeds used were chemically defined (Sartorius). Seed medium (SMD) was used during the seed train. For the N-1 perfusion previously optimized perfusion medium (PF-M), based on a FB media platform, was used (Janoschek et al., 2018).

2.2. Seed culture

For each passage, pre-warmed media (36.8 °C) was used. A cryo vial was thawed and washed with 10 mL SMD via centrifugation (190 *xg*, RT, 3 min). The cell pellet was resuspended with 10 mL SMD and transferred into a 500 mL non-baffled shake flask filled with 150 mL SMD. Cells were incubated in an incubation shaker at 36.8 °C, 7.5 % pCO_2, 85 % humidity and with an orbital motion of 120 rpm at a diameter of 50 mm (Certomat® CT plus, Sartorius). Cell passaging was conducted in total four times and done every three to four days starting at $0.2{\cdot}10^6$ c·mL^{-1} prior inoculation of the N-1 perfusion bioreactor. Moreover, the conventional seed train was extended and passaged in parallel to the N-1 perfusion as reference for the extended cell age after thaw. The first two passages after thawing contained 500 µM methotrexate hydrate (Sigma).

2.3. N-1 perfusion bioreactor based on rocking motion

Single-use bag bioreactors equipped with an internal perfusion membrane based on rocking motion (Biostat® RM 20|50, Sartorius) were used at the N-1 stage, i. e. one control and one experimental approach (RM_c and RM_e, Fig. 1). The bioreactors (V_{work}: 1 L) were inoculated at $0.2{\cdot}10^6$ c·mL^{-1} in SMD in batch mode. Cultivation parameters were set to 36.8 °C, 60 % DO, pH 7.1 controlled by CO_2 gassing at an overall gas flow rate of 0.03 L·min^{-1}. The rocking rate was set to 30 rpm with an angle of 10°.

In order to determine the VCC online, measurements of the biocapacitance were obtained using a single-use impedance probe (BioPAT® ViaMass, Sartorius) attached to the RM bag. Single frequency measurements were performed at 580 kHz. A linear regression factor *k* based on empirical data specific for both cell line and medium was used to convert the measured permittivity $\Delta\varepsilon$ directly into the online VCC. Thus, relative changes in the permittivity reflect growing cells.

$$VCC = k{\cdot}\Delta\varepsilon \quad (1)$$

The online VCC was then used to start the perfusion as soon as $2.5{\cdot}10^6$ c·mL^{-1} were reached and to adjust the PR automatically based on different CSPR setpoints with a feedback control. Simultaneously, the pH was shifted to 6.95 to minimize usage of 1 M Na_2CO_3, that was additionally used if needed, at high cell densities and respectively increased total cellular CO_2 emission. DO control of 60 % by head space aeration was started automatically by increasing the rocking rate if required. The N-1 perfusion processes lasted over seven days and were separated into different consecutive phases. Initially, (1) a constant PR of 1 vvd was used to exchange remaining SMD directly with PF-M. As soon as a CSPR of 50 pL·(c·d)$^{-1}$ was reached (2), the PR was controlled

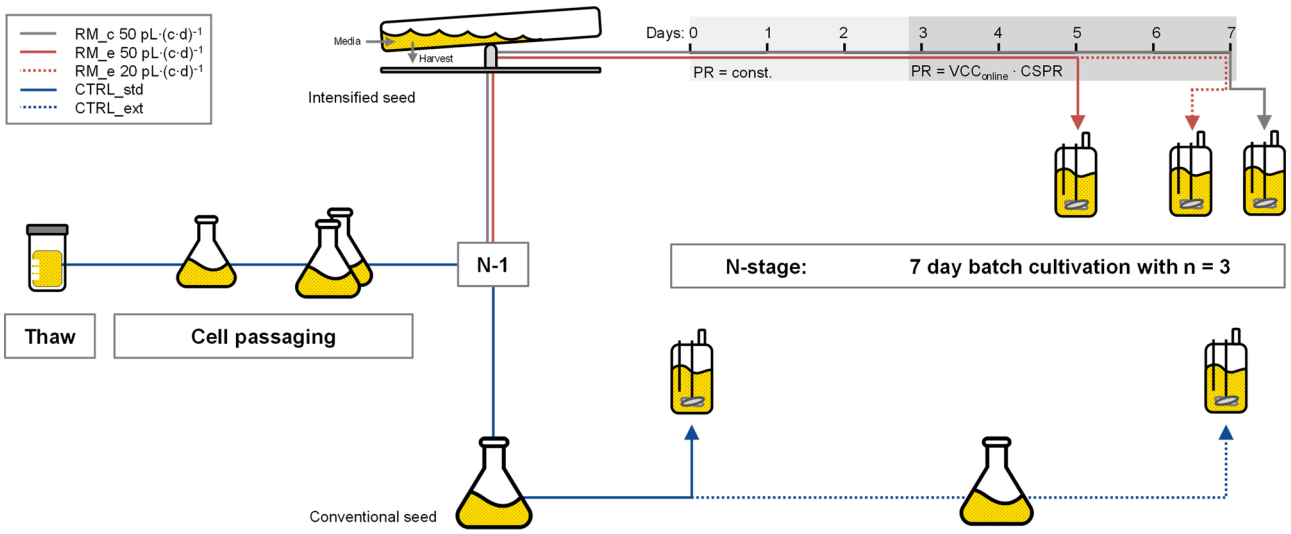

Fig. 1. Study design for the investigation of automated online CSPR control at N-1 perfusion and its impact on subsequent N-stage batch processes: Cells were thawed and expanded regularly up to the N-1 stage, where they were separated into intensified and conventional seeds. A control N-1 perfusion (RM_c) was maintained at a CSPR of 50 pL·(c·d)$^{-1}$ for 7 days and was compared against an experimental approach (RM_e) with a lower CSPR of 20 pL·(c·d)$^{-1}$ from day 5 ongoing. A conventional seed train (CTRL_std) was used as reference including an approach with an extended number of passages (CTRL_ext) to account for increased cell age after thaw.

automatically. For the control N-1 perfusion (RM_c) 50 pL·(c·d)$^{-1}$ were maintained until the end. For the experimental N-1 perfusion (RM_e), the CSPR setpoint was (3) set to 20 pL·(c·d)$^{-1}$ from day 5 until the end.

The cultivations were sampled up to three times per day (4 mL). Samples were used for offline analysis as well as to store centrifuged (15,000 *xg*, RT, 5 min) supernatants at −20 °C for subsequent IgG quantification and spent media analysis.

2.4. N-stage production bioreactor in multiparallel, automated small-scale bioreactors

The automated small-scale bioreactor system Ambr®15 with sparged cell culture vessels (Sartorius) was used in this experiment as N-stage bioreactors to evaluate the quality of different inocula according to Table 1 in batch cultures lasting for seven days. Each vessel was inoculated at 0.3·10^6 c·mL^{-1} and a starting volume of 15 mL. Thus, the required inoculation volumes varied by about factor 30 with 1.5 and 0.05 mL used from conventional (3·10^6 c·mL^{-1}) and perfusion N-1 (day 7, 100·10^6 c·mL^{-1}), respectively. The temperature was set to 36.8 °C and the pH was maintained at 7.1 via CO_2 gassing. Each vessel was agitated at 1050 rpm and the DO was controlled at 60 %, while air was used as transport gas at 150 µL·min^{-1}. To prevent foaming 20 µL antifoam (2 % Antifoam C, Sigma) were added every second day. Daily samples from each vessel (700 µL) were used for offline analytics. The remaining sample volume was centrifuged (15,000 *xg*, RT, 5 min) and the supernatant was stored at −20 °C for quantitative and qualitative product analysis.

Table 1
Overview of the characteristics of the N-stage approaches.

Approach	Seed source	Days after thaw	Days at N-1 perfusion	CSPR (pL·(c·d)$^{-1}$)
CTRL_std	Conventional	16	/	/
CTRL_ext	Conventional	23	/	/
High CSPR_1	Perfusion (RM_e)	21	5	50
Low CSPR	Perfusion (RM_e)	23	7	20
High CSPR_2	Perfusion (RM_c)	23	7	50

2.5. Offline analytics

Cell growth (VCC, viability and average cell diameter d_{cell}) were measured using a Cedex HiRes Cell Counter (Roche). Based on this, the viable cell volume (*VCV*) was calculated.

$$VCV = \frac{4}{3}\cdot\pi\cdot VCC\cdot\left(\frac{d_{cell}}{2}\right)^3 \quad (2)$$

The pH, pO_2, pCO_2 as well as metabolite levels (glucose, lactate, ammonia and L-glutamine) and osmolality were measured using a Bio-Profile® FLEX2 (Nova Biomedical). Flow cytometry (iQue® Screener Plus, Sartorius) was used to measure apoptotic markers during the N-1 perfusion (RM_e) with the MultiCyt® 4-Plex Apoptosis Kit (Sartorius) according to the protocol supplied with the kit.

Spent media was measured for extracellular sugars, amino and organic acids using NMR (Spinnovation Biologics BV). The product titer was determined via HPLC using a Dionex UltiMate 3000 HPLC System (Thermo Scientific) and a Yarra 3 µm SEC 3000 (Phenomenex). Final product quality profiles from the N-stage cultivations in terms of N-Glycan profiles were analyzed using capillary electrophoresis on a microchip (LabChip® GXII^{TM} Touch 24, PerkinElmer). Samples were denatured, digested via PNGase F and stained according to the manufacturer's protocol (Glycan Profiling Assay Release and Labeling Kit, PerkinElmer).

2.6. Cell-specific rates

The cell-specific growth rate was calculated as follows:

$$\mu = \frac{\ln\left(\frac{VCC_i}{VCC_{i-1}}\right)}{\Delta t} \quad (3)$$

Based on online VCC measurements for the N-1 perfusion, the average µ (d^{-1}) was calculated for phases 2 (50 pL·(c·d)$^{-1}$) and 3 (20 pL·(c·d)$^{-1}$) as soon as three bioreactor volumes were exchanged at the corresponding CSPR to ensure steady-state conditions, i. e. at the end of each phase.

Based on the extracellular measurements of the spent media, compound balances were used to calculate the amount of a compound $\Delta n_{S,i}$ (mol) that was consumed or produced in the N-1 perfusion bioreactor:

$$\Delta n_{S,i} = \overline{PR}_i \cdot V_w \cdot \left(c_{S,Feed} - c_{S,i}\right) \cdot \Delta t_i \quad (4)$$

where V_w (L) is the working volume, PR_i (d^{-1}) is the averaged PR, $c_{S,Feed}$ the concentration of a compound in the feed and $c_{S,i}$ ($mol \cdot L^{-1}$) is the corresponding linearly averaged concentration in a certain interval Δt_i (d).

The total integral viable cells (IVC_i; cells·d) were calculated for the complete process and were used to calculate the metabolic exchange rate $q_{x,i}$ ($mol \cdot (c \cdot d)^{-1}$) for each compound within a given interval.

$$IVC_i = \sum_{i=1}^{n} \frac{VCC_i + VCC_{i-1}}{2} \cdot \Delta t_i \cdot V_w \quad (5)$$

$$q_{S,i} = \frac{\Delta n_{S,i}}{\Delta IVC_i} \quad (6)$$

Again, rates were calculated towards the end of phases 2 and 3 as mentioned above. Based upon, yield coefficients for lactate from glucose and ammonia from glutamine were calculated. In order to consider measurement deviations of both cell counting and spent media analysis (NMR), technical errors of 10 and 5 % were used for error propagation, respectively.

For the N-stage processes, cell-specific growth rates were calculated using Eq. (1) based on offline VCC measurements. Cell-specific productivities were calculated with Eq. (6) on a per cell or per cell-volume basis using the IVC or the integral viable cell volume (IVCV), respectively.

3. Results

In order to investigate and compare the effect of two different CSPRs in N-1 perfusion cultivations on cellular responses and their subsequent translation into N-stage processes, two RM 2 L bioreactors (RM_c and RM_e) were operated in perfusion mode. They were equipped with a capacitance sensor for online control of the PR. For RM_e, the CSPR setpoint was lowered during the process, while it was kept constant for RM_c as a control approach.

3.1. Cell performance at N-1 perfusion

The conducted N-1 perfusion processes (Fig. 2) were characterized by sustained strong cell growth, thus reaching a very high VCC of $100 \cdot 10^6$ $c \cdot mL^{-1}$ within seven days. For both approaches, the viability was high until then end and was only slightly reduced towards 96 % at day 7. The initial difference of 1 µm in cell diameter between the two approaches resulted very likely from the fact that separate seed trains prior inoculation of N-1 were used. Intermediate differences in both VCC and diameter between the two approaches balanced out with time explaining similar net gain in cell volume. Accurate online measurements of these high cell numbers were performed using a capacitance probe both in terms of VCC and VCV (Fig. 3). Based on the VCC measurement, the CSPR was maintained at 50 $pL \cdot (c \cdot d)^{-1}$ as soon as the initial PR of 1 d^{-1} did not suffice anymore. For RM_c it was kept at 50 $pL \cdot (c \cdot d)^{-1}$ until day 7, while for RM_e it was lowered at day 5 to 20 $pL \cdot (c \cdot d)^{-1}$ to create two subsequent, different physiological conditions (Fig. 2b) in the bioreactor.

3.2. Metabolic profiles and cell-specific rates in N-1 perfusion

Extracellular concentrations of the main energy sources glucose and glutamine as well as byproducts lactate and ammonia (Fig. 4) were measured to evaluate their dependence from the CSPR. Due to the onset of perfusion, both glucose and glutamine were initially increased, while accumulated by-products lactate and ammonia were washed out in the first phase. Reaching a constant CSPR of 50 $pL \cdot (c \cdot d)^{-1}$ allowed to establish steady-states for both processes, which were maintained for

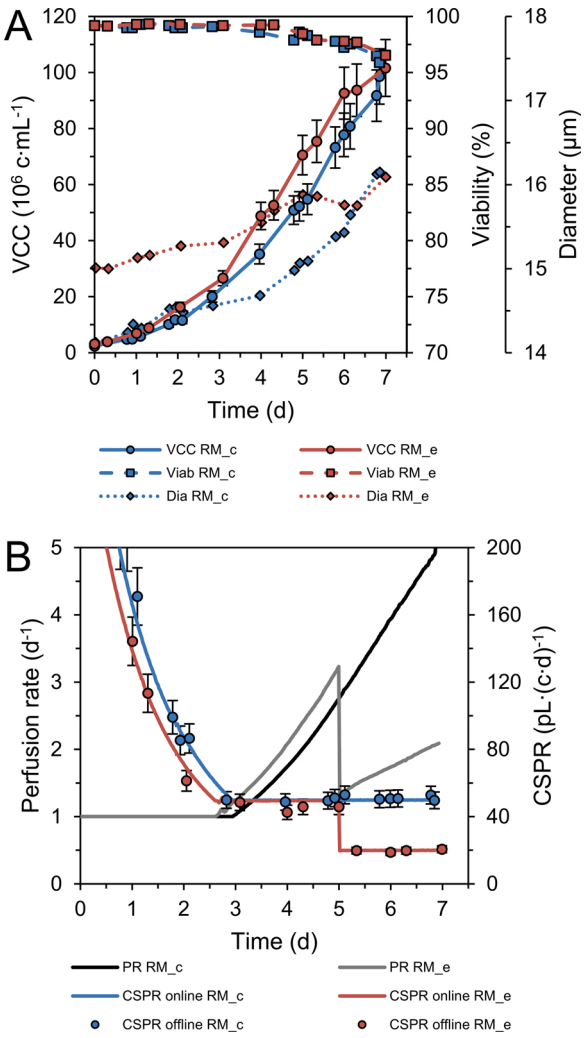

Fig. 2. Performance comparison of N-1 perfusion rocking motion seed bioreactors with RM_c and RM_e: (A) VCCs, viabilities and average cell diameters. (B) Profiles of applied perfusion rates and CSPR setpoints compared for off- and online measurements. Error bars represent 10 % technical deviation of cell counting.

the control approach until day 7. For the experimental approach, lowering the CSPR to 20 $pL \cdot (c \cdot d)^{-1}$ at day 5 caused nutrient depletion. Moreover, further analysis of the spent media of this approach (Fig. 5) revealed depletion of glutamic acid, arginine and cystine. Conversely, glycine accumulated towards the end of the process. As succinic acid is present in the perfusion media, its concentration was increased during the first phase to 6.8 mM. During the second phase all concentrations of the organic acids were constant, whereas during the final phase especially formic (5.3 mM), but also isovaleric and butyric acid (0.8 mM), accumulated due to the lowered overall PR.

Based upon the concentration profiles of the experimental N-1 perfusion approach, cell-specific metabolic exchange rates were calculated for the two different phases to understand how the metabolism responds towards the two different CSPRs. For all measured components, the uptake rates at a high CSPR (d5) were higher compared with the low CSPR (d7). The main energy sources glucose and glutamine were reduced by about 20 % and 50 %, while the formation of lactate and ammonia was decreased by 75 % and 54 %, respectively from d5 to d7 (Fig. 6a). Consequently, the lactate yield from glucose was reduced by two-third, while the ammonia yield from glutamine remained constant (Table 2). The uptake rates for all essential amino acids (Fig. 6b) were reduced by about 30 %, whereas some non-essential amino acids

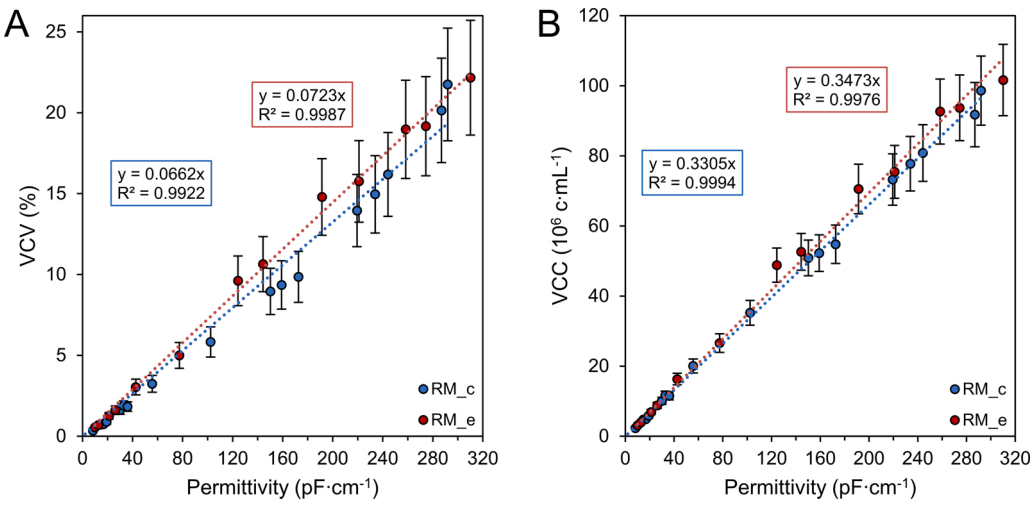

Fig. 3. Correlation of measured permittivity with offline measured (A) relative viable cell volume and (B) VCC in N-1 perfusion processes.

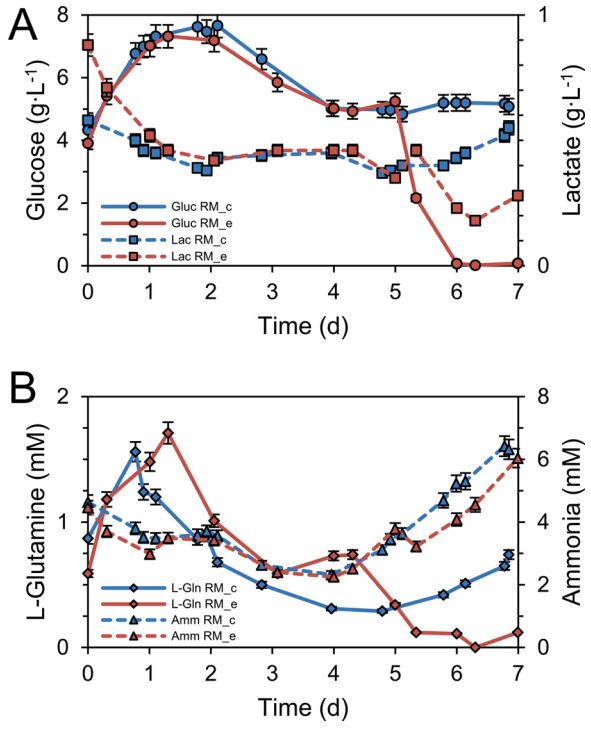

Fig. 4. Concentration profiles for (A) glucose and lactate as well as (B) L-Glutamine and ammonia during N-1 perfusion at a CSPR of 50 pL·(c·d)$^{-1}$ for RM_c respectively 20 pL·(c·d)$^{-1}$ for RM_e from day 5 ongoing. Error bars represent 5 % technical deviation of spent media analysis (NMR).

(Fig. 6c) showed different changes. Asparagine uptake was only reduced by 10 % and while cellular production of alanine was stopped, glycine production remained constant. Both formation of organic acid byproducts (citric and formic acid) as well as consumption of organic acids present in the medium (acetic and succinic acid) were reduced (Fig. 6d).

3.3. Measurement of apoptotic parameters

Next to the calculation of metabolic rates, flow cytometry was used to measure and quantify apoptotic markers as cellular response towards a limiting CSPR. In Fig. 7 the intensity of annexin V binding to externalized phosphatidylserines (PDS) located at the outer cell membrane is plotted against the intensity of the mitochondrial membrane potential (MMP) for day 5 and day 7. No apoptotic populations were formed under the high CSPR, while this was clearly observable for the low CSPR. The apoptotic response is characterized by the initial formation of a transient population with cells exhibiting decreased MMP (4.65 %) followed by an increased staining of PDS, i. e. apoptotic population (3.35 %) at day 7.

3.4. Performance at N-stage cultivation

Five inocula with different origins were used for the inoculation of batch cultivations in small-scale bioreactors being the N-1 process strategy (conventional vs. intensified), respective conditions (high and low CSPR, i. e. 50 and 20 pL·(c·d)$^{-1}$) as well as cell age after thaw (Table 1). They were assessed for their cell growth performance, productivity and product quality.

Depending on the inoculum source, there were distinct differences found for the cell growth (Fig. 8a, b). Initial cell growth at day 1 was reduced for all approaches inoculated from intensified N-1 seeds, but with a reduction to 62 % clearly more for the approach at low CSPR. During the following days, all intensified N-1 approaches showed increased cell growth, in particular and still at day 5, resulting in similar peak VCCs for all approaches between 8.07±0.35·10^6 c·mL^{-1} (low CSPR) and 8.86±0.38·10^6 c·mL^{-1} (CTRL_std). Furthermore, cellular viabilities were also affected in the beginning of the batch cultivations (Fig. 8c). While none of the control nor the high CSPR approaches showed initial viabilities below 92 %, the low CSPR approach was started with a low average viability of 87 % that furthermore dropped the day after towards 84 % and did not recover until day 4. At the same time, the cell diameter of low CSPR was increased until day 5 (Fig. 8d). This behavior was also found for the approaches using a high CSPR at N-1, but only during the first two days. While highest cell-specific glucose consumption was found directly after inoculation at day 1 for control and high CSPR approaches, it was obtained with one day delay for the low CSPR approach (Fig. 8e). Accordingly, the shift from lactate production to consumption was delayed as well (Fig. 8f).

Despite the differences in initial cell growth, the final product titer at day 7 of each respective batch approach did not vary much as listed in Table 3. Considering the corresponding final IVCCs, the average cell-specific productivities q_P were found to be higher for the intensified than for standard inocula. Overall, the highest q_P was found for the approach low CSPR which can be explained from the increased cell size until day 5. In general, cell-volume specific productivity was increased for all approaches inoculated from N-1 perfusion over control approaches. Product quality analysis in terms of the average N-glycosylation profile revealed no differences in the relative distribution as shown

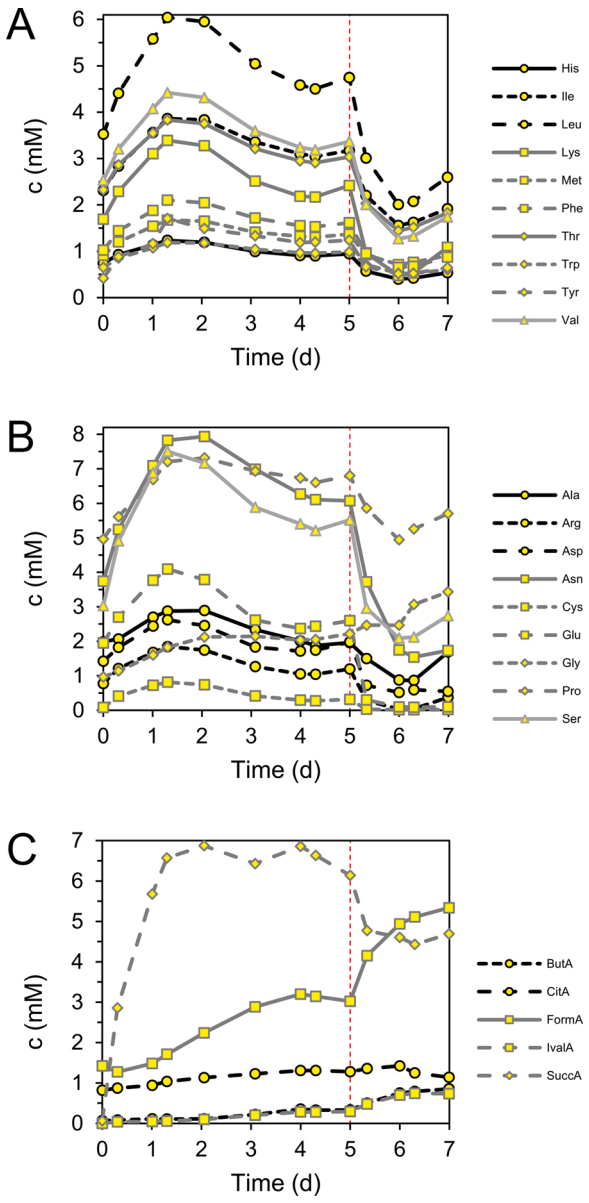

Fig. 5. Course of (A) non-essential, (B) essential amino acids and (C) organic acids (ButA: butyric, CitA: citric, FormA: formic, IvalA: isolvaeric, SuccA: succinic acid) for RM_e using two CSPR setpoints: 50 pL·(c·d)$^{-1}$ until day 5 followed by 20 pL·(c·d)$^{-1}$ until day 7 indicated by the dotted red line. Error bars (on average 5 %) are not shown for clarity of the figure. (For interpretation of the references to colour in this figure legend, the reader is referred to the web version of this article).

in Fig. 8.

4. Discussion

During the past decade, process intensification in mammalian biomanufacturing was demonstrated, amongst others, using N-1 perfusion processes to generate high cell density inocula for subsequent N-stages, thus reducing the size of the N-1 bioreactor. Depending on the CHO cell line, media composition and systems used, reports about final VCCs at the N-1 stage range from 15.8·10^6 c·mL^{-1} (Pohlscheidt et al., 2013) up to 100·10^6 c·mL^{-1} (Xu et al., 2020b). Since recently, online biomass measurement in perfusion processes is more and more used to control the PR automatically online and thus became a powerful tool (Wolf et al., 2019; Xu et al., 2020b, a; Yang et al., 2014). In the presented study, the relevance of a precise online controlled CSPR and the impact of working below its critical value in an N-1 perfusion process on the subsequent N-stage was investigated (Fig. 9).

4.1. Online perfusion rate control

An inherent characteristic of perfusion processes is the establishment of steady-state conditions in terms of process parameters, such as concentrations of nutrients, metabolites and inhibiting substances as well as the osmolality. In such a state a consistent cell physiology can be expected in terms of the cell growth and viability as well as the gene expression profile (Stepper et al., 2020). Maintaining high viabilities and a consistent cell diameter allows to measure the permittivity at a single capacitance frequency as its signal correlates primarily with the VCV instead of the VCC (Downey et al., 2014; Metze et al., 2020). Nonetheless, accurate correlations between permittivity and VCCs as well as VCVs are required for N-1 perfusion processes in order to control the CSPR robustly and reliably up to very high VCCs. Reports about the extent of this correlation in mammalian processes are available for VCCs $< 30{\cdot}10^6$ c·mL^{-1} (Downey et al., 2014; Metze et al., 2019; Opel et al., 2010), but scarce for perfusion processes with high VCCs at 100·10^6 c·mL^{-1}. They were shown occasionally up to 80·10^6 c·mL^{-1} (Mercier et al., 2016), although the technology itself is already frequently applied in different perfusion processes (Karst et al., 2016; Wolf et al., 2019; Xu et al., 2020b, a; Yang et al., 2014). In this study, the relative change of the cell diameter of about 2 µm (Fig. 2) did not contribute to a significant change of the VCV over the process time of seven days. Thus, a very high correlation between permittivity and the VCV of up to 22 % biomass as well as the VCC of up to 100·10^6 c·mL^{-1} was found (Fig. 3) emphasizing the suitability of capacitance sensors for N-1 perfusion processes. Similar results were reported for a perfusion process using a PERC.6 cell line (Mercier et al., 2016) underlining that cell size increases of up to 2 µm do not need to be accounted for when using linear regression between permittivity and VCC. Larger changes in the cell size during a process, e.g. during fed-batches with cell size increases > 4 µm (Metze et al., 2019; Pan et al., 2017, 2017), combined with an altered cell physiology towards the end of the process require multivariate data analysis of multifrequency scanning instead (Metze et al., 2020).

4.2. Impact of the CSPR on cellular responses at N-1 perfusion

Applying a constant CSPR of 50 pL·(c·d)$^{-1}$ based on the online biomass measurements in the control N-1 perfusion allowed to generate a steady state, so that cells appropriate for inoculation can be expected. This demonstrates the benefit of this feeding per cell approach which was maintained constant in a continuous way throughout the process. PR control without using online capacitance sensor would require a defined flow profile, either step-wise or continuous, which cannot consider individual cell growth of each run. In the case of the experimental N-1 perfusion, differentially treated cells for the inoculation were generated by lowering the CSPR from 50 towards 20 pL·(c·d)$^{-1}$. These cells were characterized by distinctly different cell physiological responses, although at first sight primary physiological parameters were still very comparable at day 7 (Fig. 2) when cells were used for inoculation. Based on spent media analysis, nutrients were assessed to determine their potential limitation or depletion as well as accumulation (Fig. 4) in the two phases and to identify metabolic adaptations (Fig. 5) generated from such. At a high CSPR of 50 pL·(c·d)$^{-1}$, none of the nutrients were limiting and constant levels were obtained until day 5. At a low CSPR of 20 pL·(c·d)$^{-1}$, concentrations of all nutrients were distinctly reduced by cellular consumption until day 7. Despite these very low concentrations in the second phase, the cells were, to a certain extent, still exposed to fresh nutrients due to the continuous, but relatively small, PR potentially delaying the direct response towards nutrient depletion as it would occur in discontinuous processes with full and final depletion. This can also be recognized as the cells were still forming

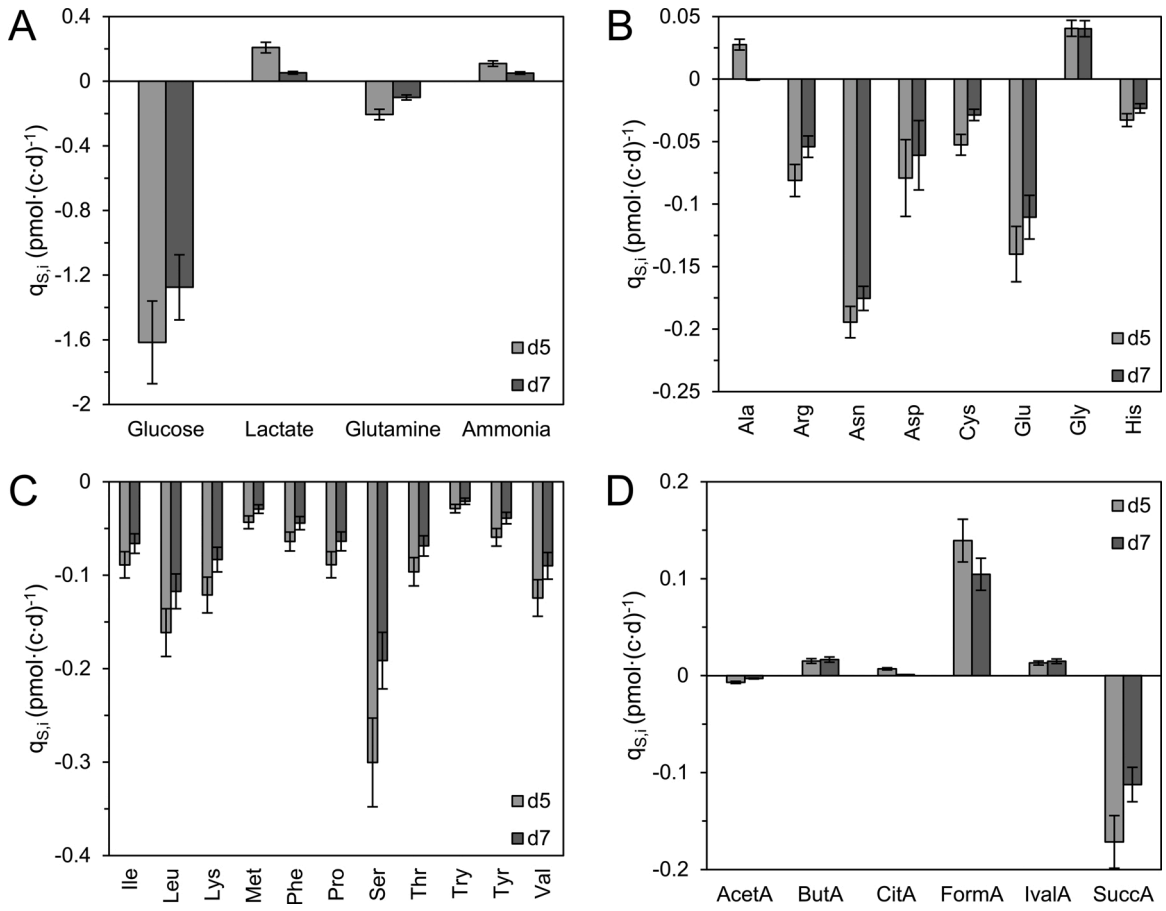

Fig. 6. Cell-specific metabolic rates at days 5 (high CSPR = 50 pL·(c·d)$^{-1}$) and 7 (low CSPR = 20 pL·(c·d)$^{-1}$) of RM_e when cells were used for the inoculation of subsequent N-stage processes: (A) glucose, lactate, glutamine and ammonia, (B) non-essential amino acids, (C) essential amino acids and (D) organic acids. Error bars represent deviations based on error propagation considering errors of 10 % on cell counting and 5 % on NMR spent media analysis.

Table 2
Growth rates and yield coefficient for lactate from glucose and ammonium from glutamine for respective days when cells were used from the experimental N-1 perfusion process (RM_e) for N-stage inoculation.

Time (d)	CSPR (pL·(c·d)$^{-1}$)	μ (d^{-1})	$Y_{Lac/Glc}$ (pmol·pmol^{-1})	$Y_{Amm/Gln}$ (pmol·pmol^{-1})
5	high (50)	0.44±0.08	0.13	0.53
7	low (20)	0.22±0.09	0.04	0.5

some lactate. Nonetheless, final concentrations of glucose and glutamine were found to be limiting as they were comparable to previously reported K_M values between 0.09 and 0.15 mM for glutamine (Glacken et al., 1988; Linz et al., 1997) and 0.01 M for glucose (Link et al., 2004), i. e. 1.8 g·L^{-1}, for different mammalian cell lines, respectively.

Due to these limitations, the cell's metabolism had to adapt and shifted towards an increased metabolic efficiency in order to generate sufficient energy required for a) maintenance and b) cell growth. On the one hand, this is indicated by the lower yield of lactate from glucose (Table 2) which was reduced by two thirds at a CSPR of 20 pL·(c·d)$^{-1}$. This implies a relative increase of the glycolytic flux into the TCA cycle. Similar results were recently reported by Wolf et al. (Wolf et al., 2019) for a semi-perfusion process in shake tubes with decreasing CSPRs. On the other hand, alanine formation was stopped under glutamine and glutamic acid limiting conditions at 20 pL·(c·d)$^{-1}$, which is a further indication for reduced formation of byproducts branching off from the central metabolism, i. e. in this case through transamination of pyruvate. This complies with reports about the dose-dependency of alanine formation from glutamine availability for CHO cells (Wahrheit et al., 2014). Moreover, the reduced uptake rates of glutamine and glutamic acid at 20 pL·(c·d)$^{-1}$, but constant yield coefficient of ammonia from glutamine of about 0.5, reveal sustained anaplerotic flux into the TCA cycle via deamidation thereof.

In correlation with theses metabolic shifts, the cellular growth rate was reduced by 50 % (Table 2) at 20 pL·(c·d)$^{-1}$ accompanied by an increased apoptotic response. Growth suppression due to nutrient limitation is a well-studied phenomenon in mammalian cell culture. It can be induced by the activation of the amino acid response pathway (Fomina-Yadlin et al., 2014). Further effects of this pathway can include a potential increase of the recombinant protein excretion and the induction of apoptosis (Dey et al., 2010) as was also found in this study. Another factor contributing to a reduced growth rate can be found within the accumulation of formic acid of above 4 mM from day 5 ongoing which is the concentration CHO cell growth was shown to be inhibited at (Ihrig et al., 1995). Although cell-specific formic acid production was lowered at 20 pL·(c·d)$^{-1}$, the corresponding reduced PRs of that phase did not suffice to wash it out. Furthermore, butyric and isovaleric acid are compounds known to cause cell cycle arrest which were found to accumulate at 20 pL·(c·d)$^{-1}$ as well (Coronel et al., 2016; Liu et al., 2001). For production processes, mild and targeted growth reduction, e. g. induced by nutrient limitation, can be desired to increase respective product yields (Hong et al., 2010; Kim et al., 2013). Instead, for an N-1 perfusion process as shown here, the primary goal is to generate exponentially growing and highly viable cells that continue to proliferate rapidly in the subsequent N-stage production bioreactor. For the design of such a process, the correct CSPR needs to be tested and identified considering a balanced nutrient supply as well as sufficient removal of inhibiting substances. Also, the CSPR should not be selected

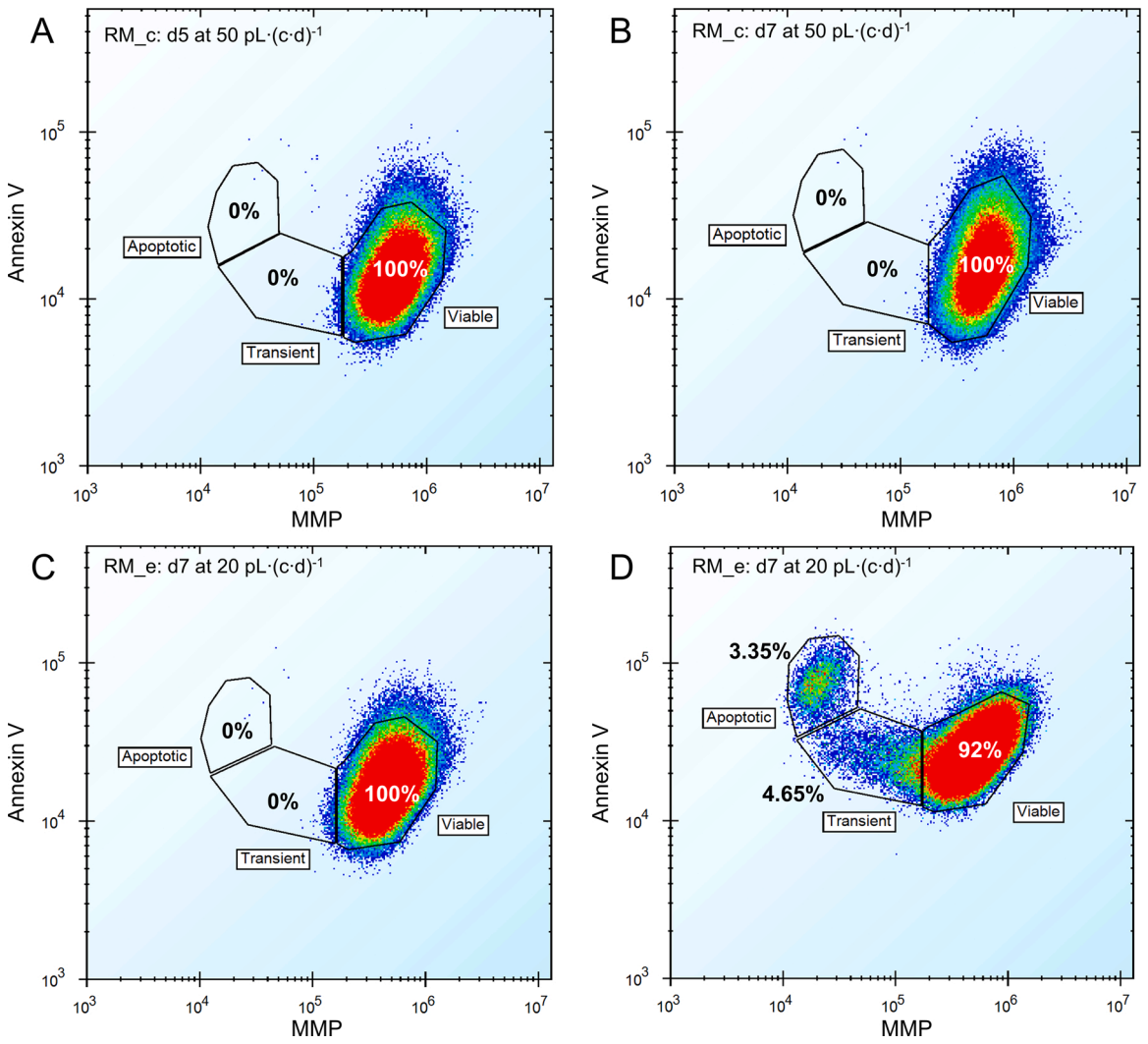

Fig. 7. Comparison of apoptoic responses towards different CSPR setpoints. Annexin V plotted against the mitochondrial membrane potential (MMP) for RM_c at (A) day 5 and (B) day 7 with constantly 50 pL·(c·d)$^{-1}$ and RM_e at (C) day 5 with 50 pL·(c·d)$^{-1}$ and (D) day 7 with 20 pL·(c·d)$^{-1}$. Populations were quantified if they contained more than 20,000 events.

too close to its critical value to add a small safety margin. Here, 50 pL·(c·d)$^{-1}$ were identified to be ideal in previous experiments (Janoschek et al., 2018), while 20 pL·(c·d)$^{-1}$ were deliberately chosen to be limiting for the given perfusion media and cell line.

4.3. Relevance and translation into N-stage

In this study, batch cultivations were used as N-stage processes to uncover cellular responses generated from conditions of the respective N-1 stage. Conventional seed trains with batch-wise passaging were used as controls. Their results showed that an extended cell age after thaw of seven days did not impact cell growth as similar peak VCCs, viabilities and cell diameters were reached. Also, the productivity remained similar. Thus, the differences found for the approaches inoculated from N-1 perfusion can be attributed to the impact of the different CSPRs. Applying the high CSPR allowed to generate comparable initial cell growth and viability compared with the approaches inoculated from the conventional seed train. For the low CSPR, initial cell growth and viability was impaired as could already be seen towards the end of the N-1 perfusion. Hence, the extended lag phase in the batch mode was extended for this approach. This was further confirmed by prolonged high glucose uptake which was enabled by lower initial cell numbers and combined with a delayed shift from lactate production to consumption. Here, the reduced initial cell growth can be a result of the increased ratio of apoptotic cells combined with decreased intracellular pools of precursors required for biomass, i. e. lipids, proteins and carbohydrates, and replication, i. e. nucleotides, as a consequence of the low CSPR.

Although similar peak VCCs were obtained after five days for all approaches due to the delayed but strong growth at day 5, the initial cell growth behavior and metabolic state during the first days of the production process is of critical importance. Fed-batch processes are most frequently used here, in which, after a short batch phase of a few days, feeding is started including defined media compositions and schedules. Hence, growth performance in this first batch phase should be high and also reproducible independent from the inoculation source to make process intensification of existing production platforms as simple as possible. In this study, a potential feed start after 3 days would have resulted in deviating feed ratios per cell as well as supply of feed compounds at different metabolic states between the approaches, thus causing inconsistencies and overfeeding.

Cell-specific IgG productivity was the highest for the approach inoculated from a low CSPR of 20 pL·(c·d)$^{-1}$. This may have been caused by the increased cell diameter until day 4. The correlation between cell size and productivity is well-known (Lloyd et al., 2000) and caused by an increased protein biosynthesis machinery in larger cells (Edros et al.,

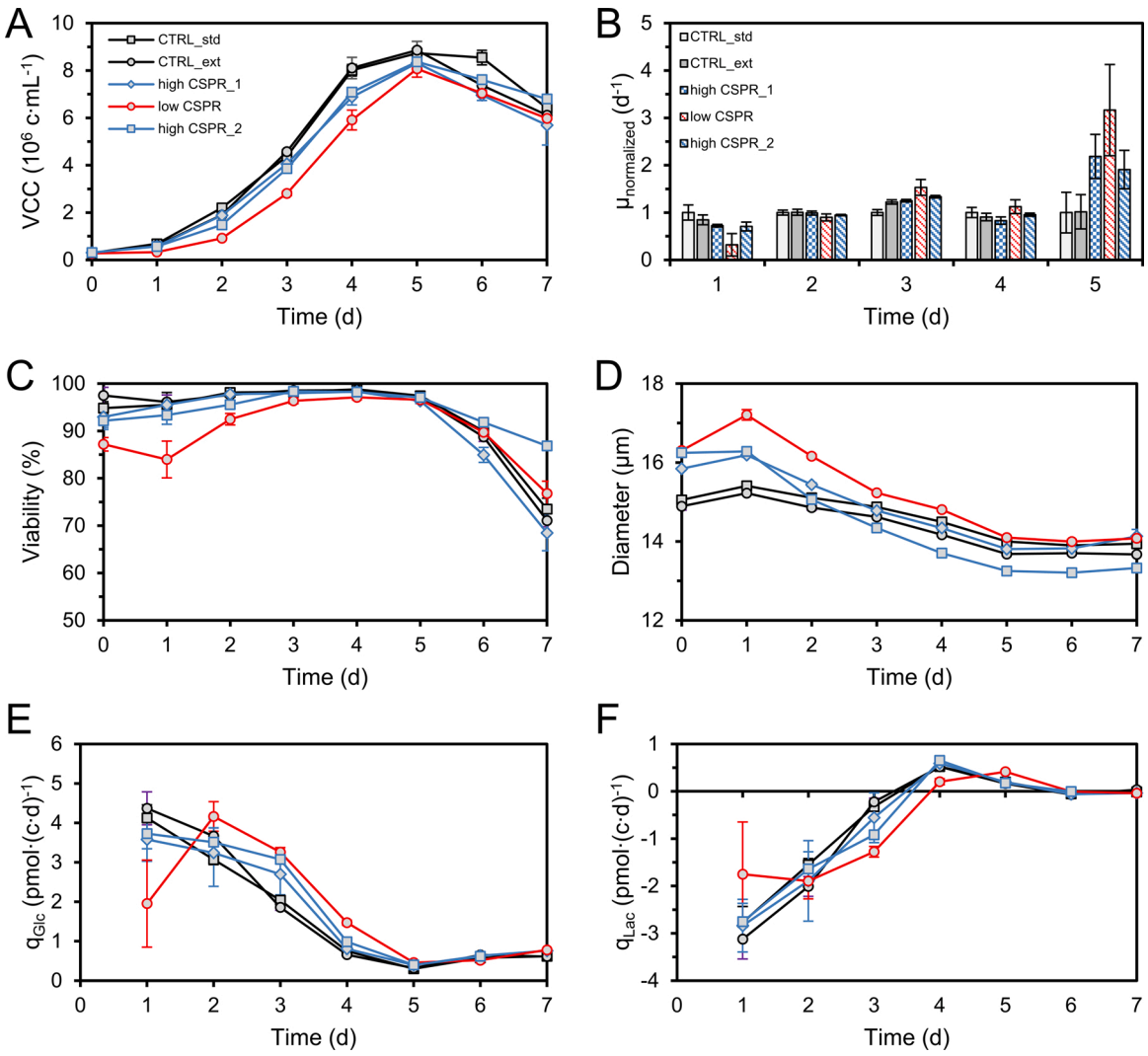

Fig. 8. Cell growth performance in batch cultivations (N-stage) inoculated from different N-1 seeds in terms of (A) VCC, (B) cell growth normalized with CTRL_std, (C) cell viability and (D) average cell diameter as well as cell-specific exchange rates for (E) glucose and (F) lactate. Each cultivation was performed triplicates, error bars represent standard deviation for each approach.

Table 3
Comparison of averaged peak VCC, total IVCC, final product titer at day 7 and averaged specific productivities for batch cultivations (n=3) inoculated from different N-1 seeds.

Approach	Peak VCC (10^6 c·mL^{-1})	Total IVCC (10^6 c·d·mL^{-1})	Final titer (mg·L^{-1})	Cell-specific productivity (pg·(c·d)$^{-1}$)	Cell-volume-specific productivity (pg·(mm^3·d)$^{-1}$)
CTRL_std	8.73±0.14	36.09±0.51	462.25±5.97	12.81±0.27	8.38±0.16
CTRL_ext	8.86±0.38	34.72±1.05	447.17±9.55	12.9±0.65	8.91±0.43
high CSPR_1	8.32±0.21	31.6±1.13	494.25±3.96	15.67±0.68	10.35±0.39
low CSPR	8.07±0.35	28.21±0.9	473.83±13.46	16.81±0.8	10.58±0.45
high CSPR_2	8.37±0.31	32.33±0.35	474.33±2.62	14.67±0.16	10.95±0.08

2014). As the quality of the produced IgG depends on the physiological state of the cells, potentially already at the end of N-1 and beginning of N-stage, theglycan profile might have changed and was therefore tested still this was not expected and was found not to be altered in this study. Also, the different cell sizes observed throughout the different approaches did not impact the glycan profile which was also reported for a fed-batch (Pan et al., 2017). As the productivities of all approaches using N-1 perfusion were, even after volume correction, generally enhanced in comparison with the control, its application seemed to favor the protein production. The potential carry-over of richer medium from the N-1 perfusion can be excluded to cause this increased productivity since the required inoculation volume compared to the conventional seeds was reduced by about a factor 30. More likely, cells from the N-1 perfusion were already exposed to the richer and more complex perfusion medium (Janoschek et al., 2018), ultimately conditioning the cells for protein production. The basal seed medium used in the conventional N-1, instead, is merely designed to support cell growth. Considering the application of a fed-batch at the N-stage would relativize this enhanced productivity due to feeding and extended process duration. For this study, batch processes were selected to observe cellular responses

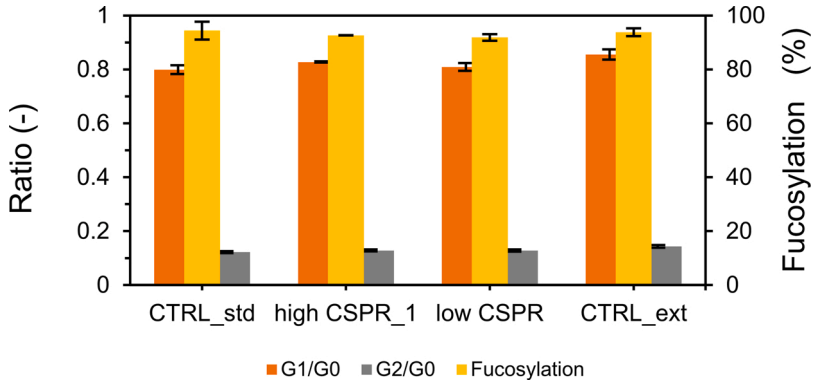

Fig. 9. N-glycosylation profiles for the IgG produced in batch cultivations (n=3) inoculated from different N-1 seeds.

pending on the conditions at the N-1 stage, while feeding would have potentially obscured them.

5. Conclusion

This study demonstrates that process intensification at the N-1 stage can be effectively achieved by implementing perfusion. The proposed strategy allows to inoculate a 2000 L bioreactor with an inoculum of 6 L from an N-1 perfusion, that can be generated with a decently small seed train bioreactor. One of the most important perfusion parameters, the CSPR, was assessed for its impact on the quality of inoculum cells, and translation into the subsequent N-stage process. VCCs of up to $100{\cdot}10^6$ $c{\cdot}mL^{-1}$ were obtained by using online biomass measurements to control the PR accurately based on a CSPR setpoint. This study showed that particular attention must be paid to the CSPR when it comes to perfusion process development as it depends on both the cell line type and medium (Konstantinov et al., 2006). Implementing a high CSPR bears the risk of inefficient medim, usage while setting it too low can result in nutrient deficiency as well as potential accumulation of inhibiting substances. In this study, using a high CSPR of 50 $pL{\cdot}(c{\cdot}d)^{-1}$ at the N-1 perfusion, performance at the N-stage was comparable to the conventional and well established N-1 stage using batch wise passaging. On the contrary, a low CSPR of 20 $pL{\cdot}(c{\cdot}d)^{-1}$ impaired inoculation quality due to nutrient depletion which was indicated by the formation of apoptotic cell populations and impaired initial cell growth at the N-stage. On the basis of these results, future work will be conducted using a CSPR of 50 $pL{\cdot}(c{\cdot}d)^{-1}$ for N-1 perfusion processes to ensure generation of high quality inocula and further extend process intensification to the N-stage by implementing intensified fed-batches. Here, integration of more detailed analysis, including transcriptomics (Stepper et al., 2020) and metabolomics, will help gaining further in-depth understanding of process intensification on the biological level.

Funding sources

This research did not receive any specific grant from funding agencies in the public, commercial, or not-for-profit sectors.

CRediT authorship contribution statement

Markus Schulze: Conceptualization, Methodology, Investigation, Formal analysis, Visualization, Writing - original draft, Writing - review & editing. **Johannes Lemke:** Conceptualization, Software, Writing - review & editing. **David Pollard:** Writing - review & editing. **Rene H. Wijffels:** Writing - review & editing. **Jens Matuszczyk:** Supervision, Methodology, Writing - review & editing. **Dirk E. Martens:** Supervision, Methodology, Writing - review & editing.

Declaration of Competing Interest

The authors report no declarations of interest.

Acknowledgment

The authors thank the complete BioProcessing team of Sartorius Stedim Biotech GmbH, without whose support this study would not have been feasible.

References

Bielser, J.-M., Wolf, M., Souquet, J., Broly, H., Morbidelli, M., 2018. Perfusion mammalian cell culture for recombinant protein manufacturing - A critical review. Biotechnol. Adv. 36 (4), 1328–1340.
Blackstone, E.A., Joseph, P.F., 2013. The economics of biosimilars. Am. Health Drug Benefits 6 (8), 469–478.
Clincke, M.-F., Molleryd, C., Zhang, Y., Lindskog, E., Walsh, K., Chotteau, V., 2011. Study of a recombinant CHO cell line producing a monoclonal antibody by ATF or TFF external filter perfusion in a WAVE Bioreactor. BMC Proc. 5 (Suppl 8), P105.
Coronel, J., Klausing, S., Heinrich, C., Noll, T., Figueredo-Cardero, A., Castilho, L.R., 2016. Valeric acid supplementation combined to mild hypothermia increases productivity in CHO cell cultivations. Biochem. Eng. J. 114, 101–109.
Dey, S., Baird, T.D., Zhou, D., Palam, L.R., Spandau, D.F., Wek, R.C., 2010. Both transcriptional regulation and translational control of ATF4 are central to the integrated stress response. J. Biol. Chem. 285 (43), 33165–33174.
Downey, B.J., Graham, L.J., Breit, J.F., Glutting, N.K., 2014. A novel approach for using dielectric spectroscopy to predict viable cell volume (VCV) in early process development. Biotechnol. Progress 30 (2), 479–487.
Ecker, D.M., Ransohoff, T.C., 2014. Mammalian cell culture capacity for biopharmaceutical manufacturing. In: Zhou, W., Kantardjieff, A. (Eds.), Mammalian Cell Cultures for Biologics Manufacturing. Springer, Berlin Heidelberg, Berlin, Heidelberg, pp. 185–225.
Edros, R., McDonnell, S., Al-Rubeai, M., 2014. The relationship between mTOR signalling pathway and recombinant antibody productivity in CHO cell lines. BMC Biotechnol. 14 (1), 15.
Fernandes, B., Correia, R., Sousa, M., Carrondo, M.J.T., Alves, P.M., Roldão, A., 2021. Integrating high cell density cultures with adapted laboratory evolution for improved Gag-HA virus-like particles production in stable insect cell lines. Biotechnol. Bioeng. n/a (n/a).
Fomina-Yadlin, D., Gosink, J.J., McCoy, R., Follstad, B., Morris, A., Russell, C.B., McGrew, J.T., 2014. Cellular responses to individual amino-acid depletion in antibody-expressing and parental CHO cell lines. Biotechnol. Bioeng. 111 (5), 965–979.
Gagnon, M., Nagre, S., Wang, W., Coffman, J., Hiller, G.W., 2019. Novel, linked bioreactor system for continuous production of biologics. Biotechnol. Bioeng. 116 (8), 1946–1958.
Glacken, M.W., Adema, E., Sinskey, A.J., 1988. Mathematical descriptions of hybridoma culture kinetics: I. Initial metabolic rates. Biotechnol. Bioeng. 32 (4), 491–506.
Hiller, G., Ovalle, A., Gagnon, M., Curran, M., Wang, W., 2017. Cell-controlled hybrid perfusion fed-batch CHO cell process provides significant productivity improvement over conventional fed-batch cultures: hybrid Perfusion Fed-Batch CHO Culture. Biotechnol. Bioeng. 114.
Hong, J.K., Cho, S.M., Yoon, S.K., 2010. Substitution of glutamine by glutamate enhances production and galactosylation of recombinant IgG in Chinese hamster ovary cells. Appl. Microbiol. Biotechnol. 88 (4), 869–876.
Ihrig, T.J., Maulawizada, M.A., Thomas, B.D., Jacobson, F.S., 1995. Formate production by CHO cells: biosynthetic mechanism and potential cytotoxicity. In: Beuvery, E.C., Griffiths, J.B., Zeijlemaker, W.P. (Eds.), Animal Cell Technology: Developments Towards the 21st Century. Springer Netherlands, Dordrecht, pp. 193–197.

Janoschek, S., Schulze, M., Zijlstra, G., Greller, G., Matuszczyk, J., 2018. A protocol to transfer a fed-batch platform process into semi-perfusion mode: the benefit of automated small-scale bioreactors compared to shake flasks as scale-down model. Biotechnol. Prog.

Jayapal, K., Wlaschin, K.F., Hu, W.S., Yap, M., 2007. Recombinant protein therapeutics from CHO cells - 20 years and counting. Chem. Eng. Prog. 103, 40–47.

Kantardjieff, A., Zhou, W., 2014. Mammalian cell cultures for biologics manufacturing. Adv. Biochem. Eng. Biotechnol. 139, 1–9.

Karst, D.J., Serra, E., Villiger, T.K., Soos, M., Morbidelli, M., 2016. Characterization and comparison of ATF and TFF in stirred bioreactors for continuous mammalian cell culture processes. Biochem. Eng. J. 110, 17–26.

Karst, D.J., Steinebach, F., Morbidelli, M., 2018. Continuous integrated manufacturing of therapeutic proteins. Curr. Opin. Biotechnol. 53, 76–84.

Kim, D.Y., Chaudhry, M.A., Kennard, M.L., Jardon, M.A., Braasch, K., Dionne, B., Butler, M., Piret, J.M., 2013. Fed-batch CHO cell t-PA production and feed glutamine replacement to reduce ammonia production. Biotechnol. Progress 29 (1), 165–175.

Konstantinov, K., Goudar, C., Ng, M., Meneses, R., Thrift, J., Chuppa, S., Matanguihan, C., Michaels, J., Naveh, D., 2006. The ⬓Push-to-Low⇼ approach for optimization of High-density perfusion cultures of animal cells. In: Hu, W.-S. (Ed.), Cell Culture Engineering. Springer Berlin Heidelberg, Berlin, Heidelberg, pp. 75–98.

Kunert, R., Reinhart, D., 2016. Advances in recombinant antibody manufacturing. Appl. Microbiol. Biotechnol. 100 (8), 3451–3461.

Link, T., Bäckström, M., Graham, R., Essers, R., Zörner, K., Gätgens, J., Burchell, J., Taylor-Papadimitriou, J., Hansson, G.C., Noll, T., 2004. Bioprocess development for the production of a recombinant MUC1 fusion protein expressed by CHO-K1 cells in protein-free medium. J. Biotechnol. 110 (1), 51–62.

Linz, M., Zeng, A.P., Wagner, R., Deckwer, W.D., 1997. Stoichiometry, kinetics, and regulation of glucose and amino acid metabolism of a recombinant BHK cell line in batch and continuous cultures. Biotechnol. Progress 13 (4), 453–463.

Liu, C.-H., Chu, I.-M., Hwang, S.-M., 2001. Pentanoic acid, a novel protein synthesis stimulant for chinese hamster ovary (CHO) cells. J. Biosci. Bioeng. 91 (1), 71–75.

Lloyd, D.R., Holmes, P., Jackson, L.P., Emery, A.N., Al-Rubeai, M., 2000. Relationship between cell size, cell cycle and specific recombinant protein productivity. Cytotechnology 34 (1-2), 59–70.

Mercier, S.M., Rouel, P.M., Lebrun, P., Diepenbroek, B., Wijffels, R.H., Streefland, M., 2016. Process analytical technology tools for perfusion cell culture. Eng. Life Sci. 16 (1), 25–35.

Metze, S., Ruhl, S., Greller, G., Grimm, C., Scholz, J., 2019. Monitoring online biomass with a capacitance sensor during scale-up of industrially relevant CHO cell culture fed-batch processes in single-use bioreactors. Bioprocess Biosyst. Eng. 43.

Metze, S., Blioch, S., Matuszczyk, J., Greller, G., Grimm, C., Scholz, J., Hoehse, M., 2020. Multivariate data analysis of capacitance frequency scanning for online monitoring of viable cell concentrations in small-scale bioreactors. Anal. Bioanal. Chem. 412 (9), 2089–2102.

Opel, C.F., Li, J., Amanullah, A., 2010. Quantitative modeling of viable cell density, cell size, intracellular conductivity, and membrane capacitance in batch and fed-batch CHO processes using dielectric spectroscopy. Biotechnol. Progress 26 (4), 1187–1199.

Pan, X., Dalm, C., Wijffels, R.H., Martens, D.E., 2017. Metabolic characterization of a CHO cell size increase phase in fed-batch cultures. Appl. Microbiol. Biotechnol. 101 (22), 8101–8113.

Pohlscheidt, M., Jacobs, M., Wolf, S., Thiele, J., Jockwer, A., Gabelsberger, J., Jenzsch, M., Tebbe, H., Burg, J., 2013. Optimizing capacity utilization by large scale 3000 L perfusion in seed train bioreactors. Biotechnol. Progress 29 (1), 222–229.

Ponce-Ortega, J.M., Al-Thubaiti, M.M., El-Halwagi, M.M., 2012. Process intensification: new understanding and systematic approach. Chem. Eng. Process. Process. Intensif. 53, 63–75.

Stepper, L., Filser, F.A., Fischer, S., Schaub, J., Gorr, I., Voges, R., 2020. Pre-stage perfusion and ultra-high seeding cell density in CHO fed-batch culture: a case study for process intensification guided by systems biotechnology. Bioprocess Biosyst. Eng.

United Nations, Department of Economic and Social Affairs, Population Division, 2019. United Nations, Department of Economic and Social Affairs, Population Division. World Population Prospects, p. 2019. Highlights. https://population.un.org/wpp/Publications/Files/WPP2019_Highlights.pdf. Accessed 25 June 2020.

Wahrheit, J., Nicolae, A., Heinzle, E., 2014. Dynamics of growth and metabolism controlled by glutamine availability in Chinese hamster ovary cells. Appl. Microbiol. Biotechnol. 98 (4), 1771–1783.

Warikoo, V., Godawat, R., Brower, K., Jain, S., Cummings, D., Simons, E., Johnson, T., Walther, J., Yu, M., Wright, B., McLarty, J., Karey, K.P., Hwang, C., Zhou, W., Riske, F., Konstantinov, K., 2012. Integrated continuous production of recombinant therapeutic proteins. Biotechnol. Bioeng. 109 (12), 3018–3029.

Wolf, M.K.F., Müller, A., Souquet, J., Broly, H., Morbidelli, M., 2019. Process design and development of a mammalian cell perfusion culture in shake-tube and benchtop bioreactors. Biotechnol. Bioeng. 116 (8), 1973–1985.

Xu, S., Gavin, J., Jiang, R., Chen, H., 2017. Bioreactor productivity and media cost comparison for different intensified cell culture processes. Biotechnol. Progress 33 (4), 867–878.

Xu, J., Rehmann, M., Xu, M., Zheng, S., Hill, C., He, Q., Borys, M., Li, Z.J., 2020a. Development of an intensified fed-batch production platform with doubled titers using N-1 perfusion seed for cell culture manufacturing. Bioresour. Bioprocess. 7.

Xu, J., Xu, X., Huang, C., Angelo, J., Oliveira, C.L., Xu, M., Xu, X., Temel, D., Ding, J., Ghose, S., Borys, M.C., Li, Z.J., 2020b. Biomanufacturing evolution from conventional to intensified processes for productivity improvement: a case study. mAbs 12 (1), 1770669.

Yang, W.C., Lu, J., Kwiatkowski, C., Yuan, H., Kshirsagar, R., Ryll, T., Huang, Y.-M., 2014. Perfusion seed cultures improve biopharmaceutical fed-batch production capacity and product quality. Biotechnol. Prog. 30 (3), 616–625.

Yang, W.C., Minkler, D.F., Kshirsagar, R., Ryll, T., Huang, Y.-M., 2016. Concentrated fed-batch cell culture increases manufacturing capacity without additional volumetric capacity. J. Biotechnol. 217, 1–11.